The Necessity of Precise Image Analysis to Explore an Interconnected 3D Cell Network

Alexandra Pacureanu

Chantal Muller
Max Langer
Jean Loic Rose

Francoise Peyrin

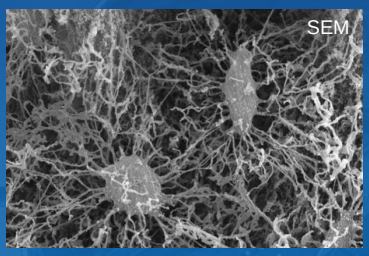

Outline

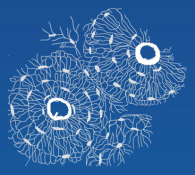

- Bone cell network
- Image acquisition
- Image enhancement
- Image segmentation
- Your input

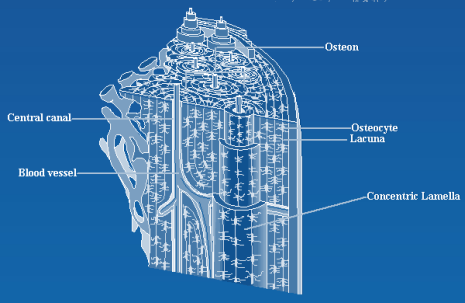

What?

- Bone: stiff and strong, yet light — Complex multiscale organization
- Dynamic tissue — Maintains and repairs itself
- Bone cell network orchestrates bone remodeling and determines bone tissue quality

- Bone composition
  - Mineral → hydroxylapatite
  - Collagen → protein

Tim Arnett, UCL

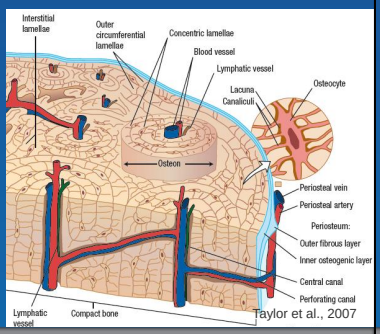

Taylor et al., 2007

Why?

- Understand bone strength, failure and mechanotransduction
- Cope with diseases:
  - Osteoporosis
  - BRONJ – jaw bone disease, cancer, etc.
- Design biomaterials – prosthesis & dental implants

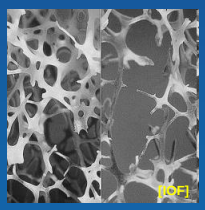

Normal Osteoporosis

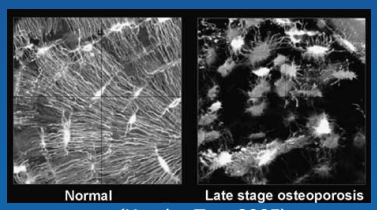

(Knothe-Tate 2005)

Trabeculae ~100 µm → Osteocytes ~300 nm

Imaging the osteocyte network

- Why is it difficult?
  - Embedded in the hard bone matrix → light can't penetrate it
  - Size of canaliculi in the range 300 – 700 nm (human) → high spatial resolution required
  - Complex 3D organization
  - Needs to be studied in a relatively large 3D region → osteon ⇔ the basic structural & functional unit in bone cortex (~200 µm diam., up to 2 mm in length)
- So far studied mainly in 2D (3D parameters infered)
- Recently – 3D methods proposed but FOV is restricted to 1-3 cells and imaging is tedious

Optical microscopy

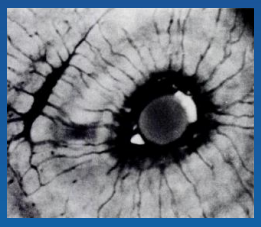

Oil immersion
(Shapiro, 1988)

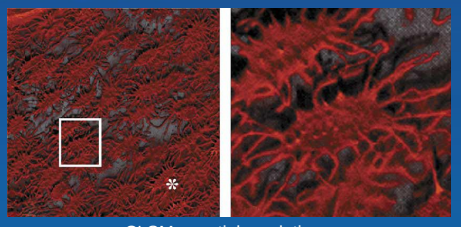

CLSM - spatial resolution
263 nm in plane
604 nm in depth
(Sugawara et al. 2005)

Electron microscopy

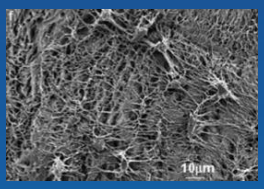

SEM of bone surface after acid-etching (Kubek et al., 2010)

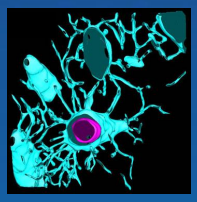

TEM (3 µm thick sections) Spatial resolution (35-50 nm) (Kamioka et al., 2009)

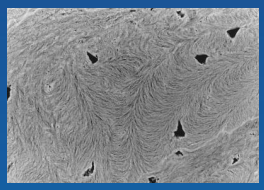

BSE-SEM (Boyde, J.Anat, 1997)

3D isotropic resolution

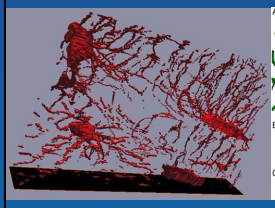

FIB-SEM (Stokes et al. 2005)

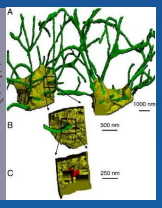

FIB-SEM (Schneider et al. 2011)

Destructive

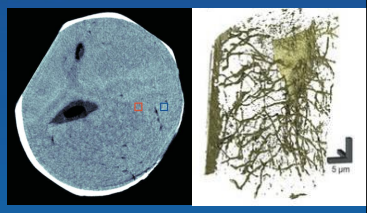

Ptychography (Dierolf et al., 2010)

Non-destructive

Why SR-microCT?

- High photon flux
- Monochromatic beam
- Large volume of view
- Parallel beam → reconstruction is exact
- Pixel size 280 nm – 30 µm

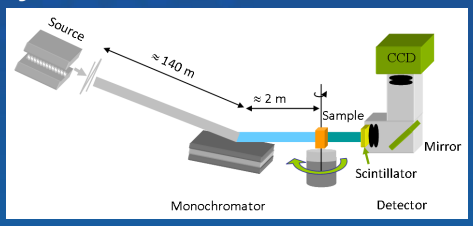

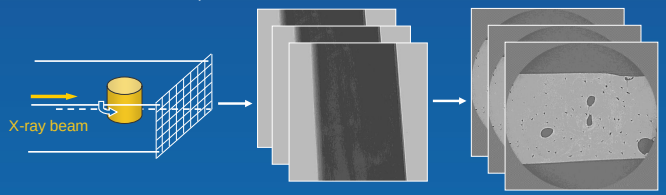

Parallel beam geometry

Record a set of projections

Reconstruct a stack of transverse slices

Imaging difficulties

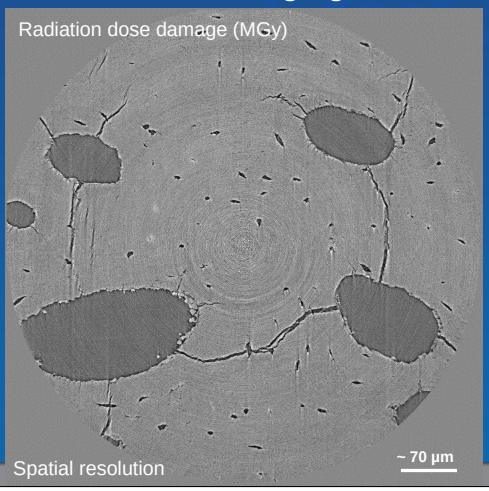

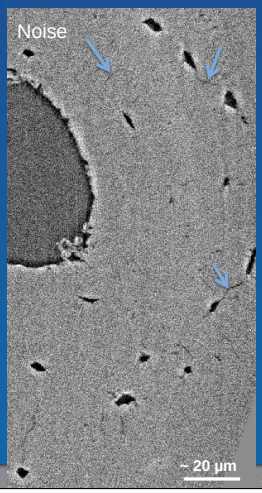

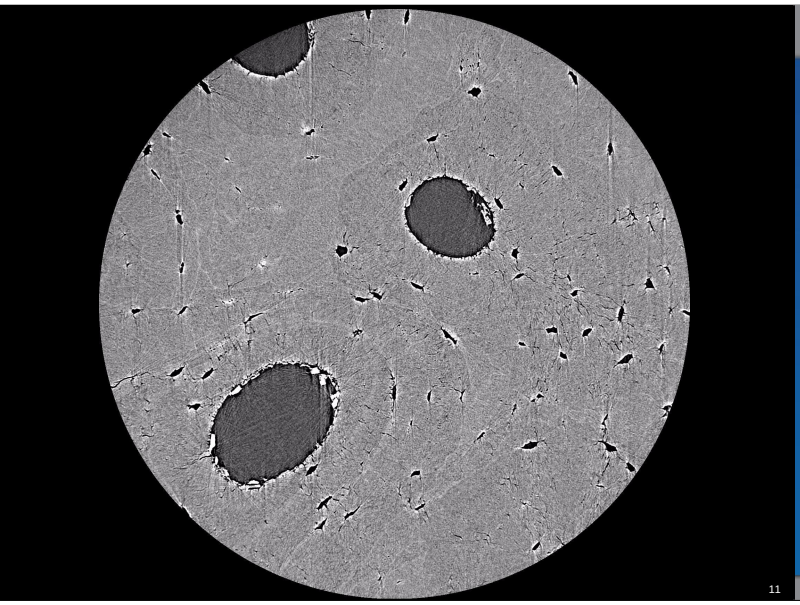

Precise image analysis is necessary

- New images – no previous work on analysing this type of structure from X-ray micro CT images
- Measurements on cell morphology, cell orientation, cell dendrites – length, branching, connectivity are needed
- Interactive segmentation not feasible (10^3 cells, 10^5-10^6 dendrites in each image)
- Some *a priori* information can be used

- Main challenges
  - Size of the canaliculi – 1-3 voxels thick in the reconstructed data
  - Partial volume effect
  - 3D complexity of the cell network
  - Bone matrix is not homogeneous
  - Noise
  - Low contrast
  - Image size – 32 GB (rescale to 8 bit => 8 GB)

Image enhancement

- Hessian based 3D line filter

$$H = \begin{pmatrix} f_{xx} & f_{xy} & f_{xz} \\ f_{yx} & f_{yy} & f_{yz} \\ f_{zx} & f_{zy} & f_{zz} \end{pmatrix}$$

Linear shape:

$$|\lambda_1| << |\lambda_2| \quad |\lambda_1| \approx 0 \quad \lambda_2 \approx \lambda_3$$

[Frangi et al.]

$$v(\mathbf{x}) = \begin{cases} 0 & \text{if } \lambda_2 > 0 \text{ or } \lambda_3 > 0 \\ (1-\exp(-\frac{R_A^2}{2a^2}))\exp(\frac{R_B^2}{2b^2})(1-\exp(-\frac{S^2}{2c^2})) \end{cases}$$

$$R_A = \frac{|\lambda_2|}{|\lambda_3|}, \quad R_B = \frac{|\lambda_1|}{\sqrt{|\lambda_2\lambda_3|}} \text{ et } S = \sqrt{\lambda_1^2 + \lambda_2^2 + \lambda_3^2}$$

R_A – ratio blob like / plate like
R_B – ratio plate like / line like

[Sato et al.]

$$I(\mathbf{x}) = \begin{cases} \exp(-\lambda_1^2 / 2(\alpha_1\lambda_c)^2) & \lambda_1 < 0, \lambda_c \neq 0 \\ 0 & \lambda_c = 0 \\ \exp(-\lambda_1^2 / 2(\alpha_2\lambda_c)^2) & \lambda_1 < 0, \lambda_c \neq 0 \end{cases}$$

$$\lambda_c = min(-\lambda_2, -\lambda_3)$$

a, b, c
α_1, α_2 → Parameters to set

Non-linear 3D line-filtering

- Combine the 3D line filter result with original image
- Related to bilateral filtering *[Smith et al, Tomasi et al.]*

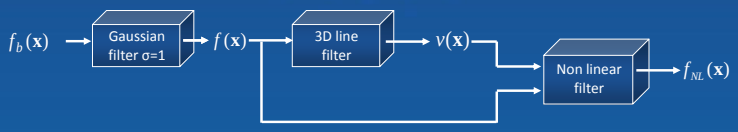

$$f_{NL}(\mathbf{x}) = \frac{1}{Z}\sum_{\mathbf{x}'\in W_{\mathbf{x}}} f(\mathbf{x}')\exp(-\frac{1}{2}(\frac{I(\mathbf{x})-I(\mathbf{x}')}{\sigma_w})^2) \text{ where } Z = \sum_{\mathbf{x}'\in W_X} \exp(-\frac{1}{2}(\frac{I(\mathbf{x})-I(\mathbf{x}')}{\sigma_w})^2)$$

$f_{NL}(\mathbf{x})$ = filtered image ; W_x = neighborhood ;
$f(\mathbf{x})$ = initial image ; $I(\mathbf{x})$ = 3D line filter map ;

- allows to recover cell lacunae and remove remaining background noise

Non-linear 3D line-filtering : results

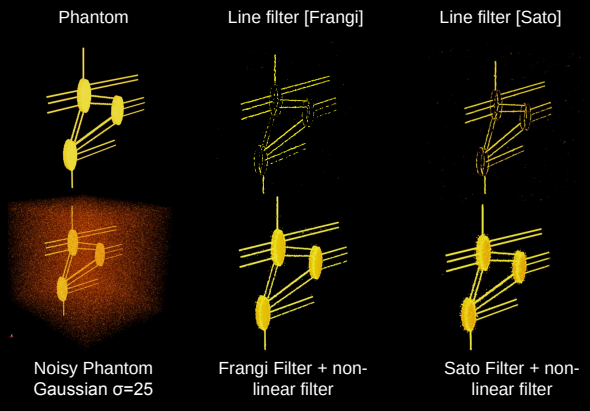

Results of the filtering on real data

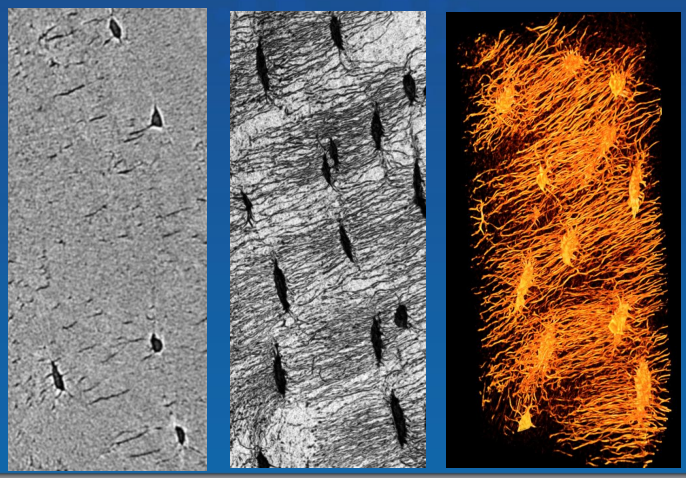

Segmentation attempts

Variational Region Growing

- Framework proposed by *[Rose, Muller et al., 2010]*
- Achieve the desired image partition by switching a discrete function $\varphi_{\mathbf{x}}$ in order to minimize a functional $J(\varphi_{\mathbf{x}})$ which models the structure to detect
- The function governing the region propagation:

$$F(\varphi_{\mathbf{x}}, \Delta J(\tilde{\varphi})) = -c(\varphi)\cdot H(-\Delta J(\tilde{\varphi}))$$

$$c(\varphi) = 1 - 2\varphi_{\mathbf{x}}$$

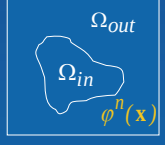

- With H, the Heaviside function
- Candidate voxels tested at each iteration – the outer border of the aggregated regions

- Design suited energy functional

Energy functional to minimize

- Inspired from Chan-Vese:

$$J_{CV}(f) = \lambda_{\text{int}} \int_{\Omega_{in}} \left| f(\mathbf{x}) - \mu_{in} \right|^2 d\mathbf{x} + \lambda_{ext} \int_{\Omega_{out}} \left| f(\mathbf{x}) - \mu_{out} \right|^2 d\mathbf{x}$$

- Use shape information from a line enhancement filter (Sato et al.)

$$J(f, v) = J_1(v) + J_2(f, v)$$

$$J_1(v) = \int_{\Omega_{in}} v(\mathbf{x}) \left| v(\mathbf{x}) - \mu_{v_{in}} \right|^2 d\mathbf{x} + \int_{\Omega_{out}} v(\mathbf{x}) \left| v(\mathbf{x}) - \mu_{v_{out}} \right|^2 d\mathbf{x} ,$$

$$J_2(f, v) = \int_{\Omega_{in}} (1 - v(\mathbf{x})) \left| f(\mathbf{x}) - \mu_{f_{in}} \right|^2 d\mathbf{x} + \int_{\Omega_{out}} (1 - v(\mathbf{x})) \left| f(\mathbf{x}) - \mu_{f_{out}} \right|^2 d\mathbf{x}$$

- $v(\mathbf{x})$ – filter response [0,1]
- Seeds generated by thresholding the line filter map.

Evaluation on synthetic image

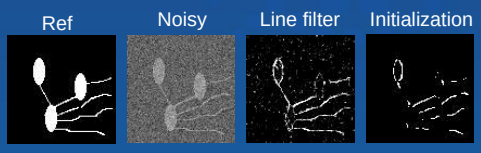

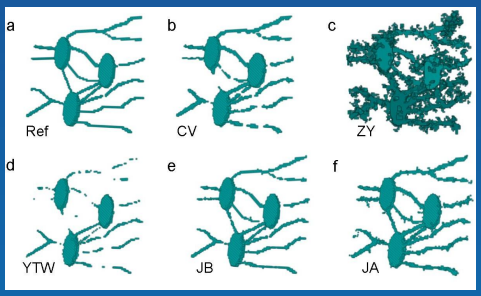

CV – gaps in dendrites

ZY – propagates too much

YTW – propagates too little

JB – performs better but some small gaps remain

JA – gives the best connectivity, but it aggregates some external voxels

Quantitative results on ground truth

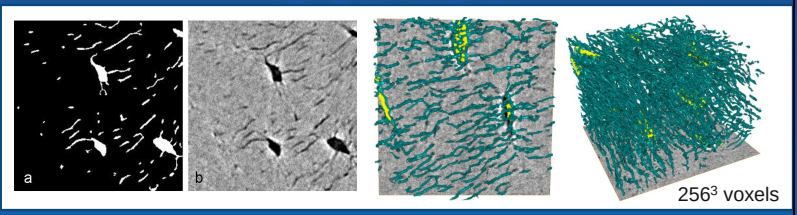

(%)	Error CC	Dice	Over-detection	Under-detection
YTW	288	74	100	59
ZY	18	56	39	96
CV	57	75	63	93
JB	21	79	67	96
JA	11	77	63	97

To address

- Fill gaps in dendrites
- Cope with branching points
- Computational costs
- Measurements – length of dendrites, branching, connectivity, etc.